Biomaterials 35 (2014) 2355–2364

Contents lists available at ScienceDirect

Biomaterials

journal homepage: www.elsevier.com/locate/biomaterials

Neuroprotective ferulic acid (FA)–glycol chitosan (GC) nanoparticles for functional restoration of traumatically injured spinal cord

Wei Wu [a,1], Seung-Young Lee [b,1], Xiangbing Wu [c,d], Jacqueline Y. Tyler [b], He Wang [b], Zheng Ouyang [b], Kinam Park [b], Xiao-Ming Xu [a,c,d,**], Ji-Xin Cheng [b,e,*]

[a] Department of Neurobiology, Shanghai Jiaotong University School of Medicine, Shanghai, PR China
[b] Weldon School of Biomedical Engineering, Purdue University, West Lafayette, IN 47907, USA
[c] Spinal Cord and Brain Injury Research Group, Stark Neurosciences Research Institute, Department of Neurological Surgery, Goldman and Campbell Brain and Spine, Indiana University School of Medicine, Indianapolis, IN 46202, USA
[d] Department of Anatomy and Cell Biology, Indiana University School of Medicine, Indianapolis, IN 46202, USA
[e] Department of Chemistry, Purdue University, West Lafayette, IN 47907, USA

ARTICLE INFO

Article history:
Received 10 October 2013
Accepted 23 November 2013
Available online 12 December 2013

Keywords:
Spinal cord injury
Neuroprotective polymer
Ferulic acid
Glycol chitosan
Functional restoration
Anti-excitotoxicity

ABSTRACT

An urgent unmet need exists for early-stage treatment of spinal cord injury (SCI). Currently methylprednisolone is the only therapeutic agent used in clinics, for which the efficacy is controversial and the side effect is well-known. We demonstrated functional restoration of injured spinal cord by self-assembled nanoparticles composed of ferulic acid modified glycol chitosan (FA–GC). Chitosan and ferulic acid are strong neuroprotective agents but their systemic delivery is difficult. Our data has shown a prolonged circulation time of the FA–GC nanoparticles allowing for effective delivery of both chitosan and ferulic acid to the injured site. Furthermore, the nanoparticles were found both in the gray matter and white matter. The *in vitro* tests demonstrated that nanoparticles protected primary neurons from glutamate-induced excitotoxicity. Using a spinal cord contusion injury model, significant recovery in locomotor function was observed in rats that were intravenously administered nanoparticles at 2 h post injury, as compared to non-improvement by methylprednisolone administration. Histological analysis revealed that FA–GC treatment significantly preserved axons and myelin and also reduced cavity volume, astrogliosis, and inflammatory response at the lesion site. No obvious adverse effects of nanoparticles to other organs were found. The restorative effect of FA–GC presents a promising potential for treating human SCIs.

1. Introduction

Few effective treatments exist for traumatic spinal cord injury (SCI) [1,2]. Difficulties in therapeutic development derived from complex temporospatial profiles of the two pathological phases of SCI: a primary mechanical injury and a subsequent secondary damage instigated by the initial trauma [3]. The primary injury, which is inclined to insult gray matter, results in immediate ischemia and energy failure by disruption of blood vessels and cell membranes, while the secondary injury is mediated by multiple neurodegenerative processes that exacerbate the primary damage [4–6]. Therefore, early repair of SCI by neuroprotective agents is critical to prevent not only temporal progression, but also spatial spread of the primary injury. Currently, methylprednisolone (MP) is the only therapeutic agent used clinically for SCI, for which its efficacy and safety are controversial [7–10].

To date, neuroprotective medicine using various biomaterials has been proposed for early SCI treatment [11–13]. The implantation of methylprednisolone (MP)-loaded poly(lactic-*co*-glycolic acid) (PLGA) nanoparticles embedded in an agarose hydrogel in an injured spinal cord allowed to sustainably and spatially release MP, resulting in decreased inflammation and lesion volume after a contusive SCI [14]. The neuroactive pentapeptide epitope, self-assembled into cylindrical nanofibers after injection into an injured spinal cord, reduced astrogliosis and cell death, and increased the number of oligodendroglia at the injury site [15]. Also, the local injection of glial cell line-derived neurotrophic factor encapsulated in PLGA nanoparticles into the injured spinal cord after contusion in rats preserved neuronal fibers and led to increase

* Corresponding author. Weldon School of Biomedical Engineering, Purdue University, West Lafayette, IN 47907, USA
** Corresponding author. Department of Neurobiology, Shanghai Jiaotong University School of Medicine, Shanghai, P.R. China.
E-mail addresses: xu26@iupui.edu (X.-M. Xu), jcheng@purdue.edu (J.-X. Cheng).
[1] Equal contribution.

0142-9612/$ – see front matter © 2013 Elsevier Ltd. All rights reserved.
http://dx.doi.org/10.1016/j.biomaterials.2013.11.074

in locomotor function [16]. Furthermore, synthetic nano-sized polymers themselves have been recently recognized as a new class of neuroprotective agents for early SCI therapy [17,18]. Local application of a high-concentration of poly(ethylene glycol) protected spinal cord tissue from reactive oxygen species and lipid peroxidation-induced damage, by repair of nerve membranes that led to restoration of compound action potential conduction and locomotor function after compression/contusion injury in adult guinea pigs [19,20]. Poloxamer 188 (P188) micelles rescued neuron cells from glutamate toxicity [21], and also improved functional outcome from SCI through aortic cross-clamping by intercalating into neuronal membranes [22]. Self-assembled monomethoxy poly(ethylene glycol)-poly(D,L-lactic acid) di-block copolymer micelles not only repaired injured axonal membranes, but also reduced calcium influx into axons, resulting in significant improvement of locomotor function after traumatic SCI in adult rats [23]. Although SCI treatment using the synthetic nano-sized polymers has demonstrated some therapeutic effects, the polymers had to be administrated within a short period of time (~15 min) after the injury, or even before the injury, to become effective. Such time windows are not clinically relevant.

Here, we report a neuroprotective nanomedicine composed of ferulic acid modified glycol chitosan, represented by the acronym FA–GC, that can restore locomotor function following traumatic SCI within a clinically-relevant therapeutic time window. Ferulic acid (FA) and glycol chitosan (GC) are both recognized as natural neuroprotective compounds [24,25]. FA, which is abundant in cell wall of commelinid plants such as rice, wheat, or in seeds of coffee, apple, peanut, *etc*., has been shown to protect neurons after cerebral ischemic injury through its anti-inflammatory, anti-oxidative, and anti-excitotoxicity effects [26–28]. The phenolic hydroxyl group in FA can absorb a hydrogen atom to form a phenoxy radical, protecting cells from oxidative stress [29,30]. Chitosan, which is produced mainly from the exoskeleton of crustaceans (*e.g.* crabs and shrimps), has proven neuroprotective effects on membrane sealing, anti-inflammatory, anti-oxidative, and anti-excitotoxicity effects as well [31–34]. It was shown that primary amines, abundant in chitosan, may play a key role in neuroprotection [35,36]. However, due to poor solubility of chitosan in an aqueous solution with neutral pH, we employed a water-soluble, glycol chitosan (GC) maintaining its neuroprotective effect derived from the primary amines in original chitosan [37].

By chemically conjugating FA to GC to form hydrophobically self-assembled nanoparticles composed of a hydrophobic FA core and a hydrophilic GC shell, our scheme significantly extends their half-life in the blood stream so that the neuroprotective effect is sufficiently realized. We determined the therapeutic effect of FA–GC nanoparticles via the Basso, Beattie and Bresnahan locomotor scale after spinal cord contusion in rats [38]. We characterized the distribution of FA–GC nanoparticles by fluorescence and stimulated Raman scattering microscopy imaging at cellular levels. We further performed histological analyses including astrogliosis, macrophage/microglia reaction, and spared axon and myelin analyses. Finally, we assessed *in vivo* toxicity of FA–GC nanoparticles via hematological and histological analyses.

2. Materials and methods

Glycol chitosan (GC) (M_w = 250 kDa; degree of deacetylation = 82.7%), trans-ferulic acid (FA), N-hydroxysuccinimide (NHS), 1-ethyl-3-(3-dimethylaminopropyl)-carbodiimide hydrochloride (EDC), HEPES sodium salt, poly-L-lysine, cytosine-β-D-arabinofuranoside, Hoechst 33342, propidium iodide (PI), and glutamate were purchased from Sigma (St. Louis, MO). The monoreactive hydroxysuccinimide ester of Cy5.5 was from Amersham Biosciences (Piscataway, NJ). Anhydrous dimethyl sulfoxide (DMSO) and methanol were purchased from Merck (Darmstadt, Germany). All other chemicals were of analytical grade, and used without further purification.

2.1. Synthesis and characterization of ferulic acid (FA)–glycol chitosan (GC) nanoparticles

Ferulic acid (FA) was conjugated to glycol chitosan (GC) at three different molar ratios of FA to GC (45, 90, and 180). Glycol chitosan (0.1 g, 4 μM) was dissolved in HEPES buffer (pH 7.5) (20 ml), followed by dilution with DMSO (10 ml), and the different amounts of ferulic acid (3.5–14 mg, 180–720 μM) were added Chemical modification was initiated by adding equal amounts (1.5-fold molar excess of ferulic acid) of EDC and NHS. The resulting solutions were stirred for 1 day at room temperature, dialyzed (molecular cutoff = 12 KDa) for 3 days against excess water/methanol (1:4 v/v), followed by dialysis against distill water, and products were lyophilized to obtain glycol chitosan conjugates with different molar ratio of ferulic acid. Synthesized conjugates were chemically analyzed using ^{1}H NMR spectroscopy (ARX-400, Bruker, Germany) and FT-IR (Nicolet NEXUS 470, Thermo). The degree of substitution, defined as the number of ferulic acid groups per one sugar residues of glycol chitosan, was determined by UV absorbance at 316 nm.

FA–GC conjugates were dispersed in PBS buffer (pH 7.4) by sonication to produce homogeneously nano-sized FA–GC nanoparticles. The sizes of FA–GC nanoparticles were determined using dynamic light scattering (DLS) (DLS, 90Plus, Brookhaven Instruments Co., NY) at 633 nm and 25 °C. The morphologies of FA–GC nanoparticles in distilled water were observed using transmission electron microscopy (TEM) (CM 200 electron microscope, Philips). Nanoparticles deposited on the grid were negatively stained with 2 wt% uranyl acetate solution. The surface charges of FA–GC nanoparticles in distilled water were determined using a zeta potential analyzer (ZetaPlus, Brookhaven Instruments Co., NY).

2.2. Cy5.5-labeled FA–GC nanoparticles

To label Cy5.5 to FA–GC polymer or GC, 1 wt % hydroxysuccinimide ester of Cy5.5 was dissolved in DMSO and mixed with FA–GC or GC solution. The reaction was performed at room temperature in the dark for 6 h. Byproducts and unreacted Cy5.5 molecules were removed over a period of two days by dialysis (molecular weight = 12 KDa) against distilled water, and the resulting product was lyophilized. The amounts of Cy5.5 in the FA–GC and GC were similar as ~0.7 wt%, as determined by Cy5.5 absorbance at 690 nm in DMSO.

2.3. Primary spinal neuron culture

Primary spinal cord neurons were obtained from Sprague Dawley rat E15 embryo spinal cords according an established protocol [39]. In brief, E15 rat spinal cords were isolated and placed in Leibovitz's L-15 medium. Meninges were carefully removed, the spinal cords were cut into small pieces and dissociated with 0.05% trypsin/EDTA for 15–20 min at 37 °C and gently triturated. After adhering at 37 °C for 30 min to eliminate glial cells and fibroblasts, neurons were plated on poly-L-lysine pre-coated 48-well plates. Neurons were incubated in a humidified atmosphere containing 5% CO_2 at 37 °C with DMEM including 10% heat-inactivated fetal calf serum, 5% heat-inactivated horse serum, and 2 mM glutamine. After 16 h, the medium was replaced with Neurobasal medium with 2% B27, 1% N2, and 2 mM glutamine. On day 3 *in vitro*, 5 μM cytosine-β-D-arabinofuranoside was added for 24 h to inhibit glia cell proliferation. Cells in 48-well plates were cultured with 200 μL medium until experimentation. With this culture protocol, a purity of greater than 87% spinal cord neuron population was obtained by 7 DIV. All experiments were performed between 7 and 10 days following initial plating.

2.4. Neuroprotective effect of FA–GC nanoparticles for in vitro glutamate-induced exitotoxicity model

The neurons were incubated with GC (0.1 mg/ml, n = 3) and FA–GC nanoparticles (0.1 mg/ml, n = 3) for 30 min, following treatment of 100 μM glutamate for 24 h. Hoechst 33342 (10 μM) was added to the culture at 37 °C for 15 min to label all cell nuclei, followed by incubation with PI (5 μg/ml) at room temperature for 10 min to stain dead cell nuclei. After staining, the medium was removed and cells were washed with 10 mM PBS, following by 10 min treatment with 4% PFA for cell fixation. The fixed cells were then washed 3 times with PBS and were ready for imaging. Images were taken by phase microscope (Olympus CK2, Japan) at 20× and 40× magnification. The cell viability was determined by counting the number of total and PI stained neuron.

2.5. Contusive spinal cord injury model

All protocols were approved by the Purdue University Animal Care and Use Committee. Adult Long-Evans rats (~300 g) were anesthetized by 90 mg/kg ketamine and 5 mg/kg xylazine. A T10 laminectomy was performed to expose the underlying thoracic spinal cord segment(s). Spinal cord contusion injury was produced using a weight-drop device developed at New York University [40]. The exposed dorsal surface of the cord was subjected to weight-drop impact using a 10 g rod (2.5 mm in diameter) dropped from a height of 12.5 mm. After the injury, the muscles and skin were closed in layers, and rats were placed on a heating pad to maintain the body temperature of the rats until they awoke. The analgestic buprenorphine (0.05–0.10 mg/kg) was administered every 12 h through subcutaneous injection for the first 3 days post-surgery for post-operation pain management.

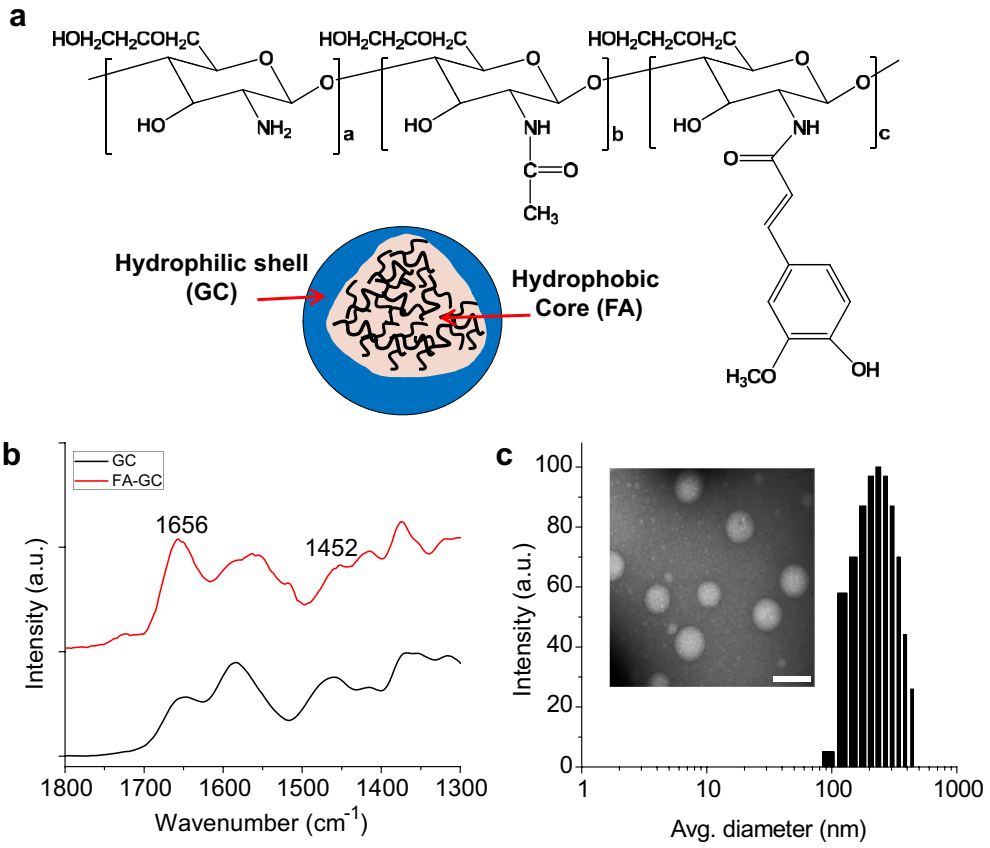

Fig. 1. FA–GC nanoparticles. (a) Chemical structure and schematic illustration of FA–GC nanoparticles. (b) FT-IR spectrum of FA–GC polymer. (c) Size distribution and TEM image of FA–GC nanoparticles (scale bar: 300 nm).

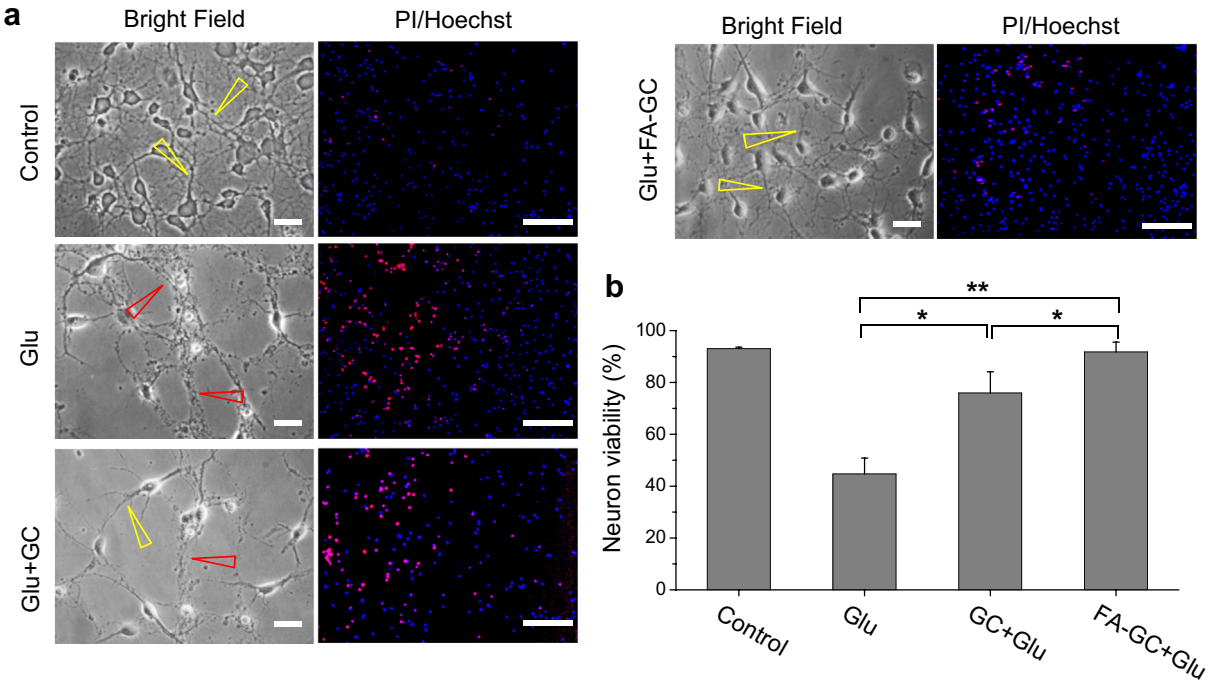

Fig. 2. Neuroprotective effect of FA–GC on primary spinal cord neurons after glutamate-induced excitotoxicity. (a, left column) Bright field images showed morphological changes of primary spinal cord neurons in treatment conditions of control, glutamate (Glu, 100 μM), Glu + GC (0.1 mg/ml) or Glu + FA–GC (0.1 mg/ml) for 24 h. Yellow and red arrows indicate intact and degenerated axons in the neurons, respectively. (a, right column) Fluorescence images of propidium iodide (PI, red, marker of dead cells) and/or Hoechst (blue, nuclear marker for both survival and dead cells) stained neurons. (b) Quantitative results of percent viability of neurons (Scale bar: 20 μm). $^{*}P < 0.05$, $^{**}P < 0.001$. (For interpretation of the references to color in this figure legend, the reader is referred to the web version of this article.)

2.6. Pharmacokinetics and tissue distribution of FA–GC nanoparticles

The pharmacokinetics of FA–GC nanoparticles and GC was determined by Cy5.5 fluorescence. FA–GC(-Cy5.5) and GC(-Cy5.5) (16 mg/kg, 1 ml in saline) were intravenously administrated to SCI rats ($n = 3$ for each group) through a jugular vein at 2 h post contusive injury ($n = 3$). Blood samples (50 μl) were drawn through another jugular vein at determined times. The fluorescence intensities of Cy5.5 labeled to FA–GC nanoparticles and GC in blood were measured by a fluorescence spectrometer (SpectraMax M5, Molecular Devices, CA) with excitation at 675 nm and emission at 695 nm. The dataset was fit to a one-compartment pharmacokinetic model:

$$y = Ae(-x/t) + y_0$$

The fluorescence imaging of FA–GC(-Cy5.5) in blood samples drawn at different time points was performed using IVIS Lumina (Caliper Life Sciences, Inc., MA) with excitation at 640 nm and emission at 695–770 nm. For biodistribution study, FA–GC(-Cy5.5) nanoparticles was intravenously injected at 2 h post injury. At 1 day after the injection, the rats were sacrificed via transcardial perfusion with saline and the tissues were harvested. Cy5.5 in the tissues was imaged by IVIS Lumina. Quantitative analysis for the tissue distribution of FA–GC nanoparticles was performed using the Living Imaging Software (Caliper Life Sciences, Inc., MA).

2.7. Nonlinear optical imaging of injured spinal cord tissue

The injured spinal cord tissue harvested in the tissue distribution study of FA–GC nanoparticles was cross-sectioned at 200 μm thickness using an oscillating tissue slicer (Electron Microscopy Sciences, Inc., PA). For simulated Raman loss (SRL) imaging, a Ti:sapphire laser (Chameleon Vision, Coherent) of 140 fs pulse duration, 80 MHz repetition rate was tuned at 830 nm to pump an optical parametric oscillator (OPO, APE compact OPO, Coherent) [41]. Based on the C–H molecular vibration, the OPO provided the Stokes beam at ~1090 nm, and then collinearly combined with the pump beam and sent to a laser scanning microscope (BX51, Olympus). The pump and Stokes beam were then focused into the sample using a water immersion objective lens (XLPlan N 25X, NA 1.05, Olympus). The forward SRL signal was collected by an oil condenser (U-AAC, NA 1.4, Olympus) and detected by a photodiode (S3994-01, Hamamatsu). The fluorescence signal was collected backward with a photomultiplier tube (H7422P-40, Hamamatsu) after an optical filter (715/60, Chroma). Pixel dwell time was 4 μs for each image.

2.8. Locomotor scoring after FA–GC nanoparticle treatment

Rats were randomly divided into 3 groups according to the treatments received: 1 ml FA–GC nanoparticles (16 mg/kg in saline; $n = 12$), 1 ml methylprednisolone sodium succinate (MP, 30 mg/kg; $n = 5$), and isovolumetric dose of saline ($n = 12$).

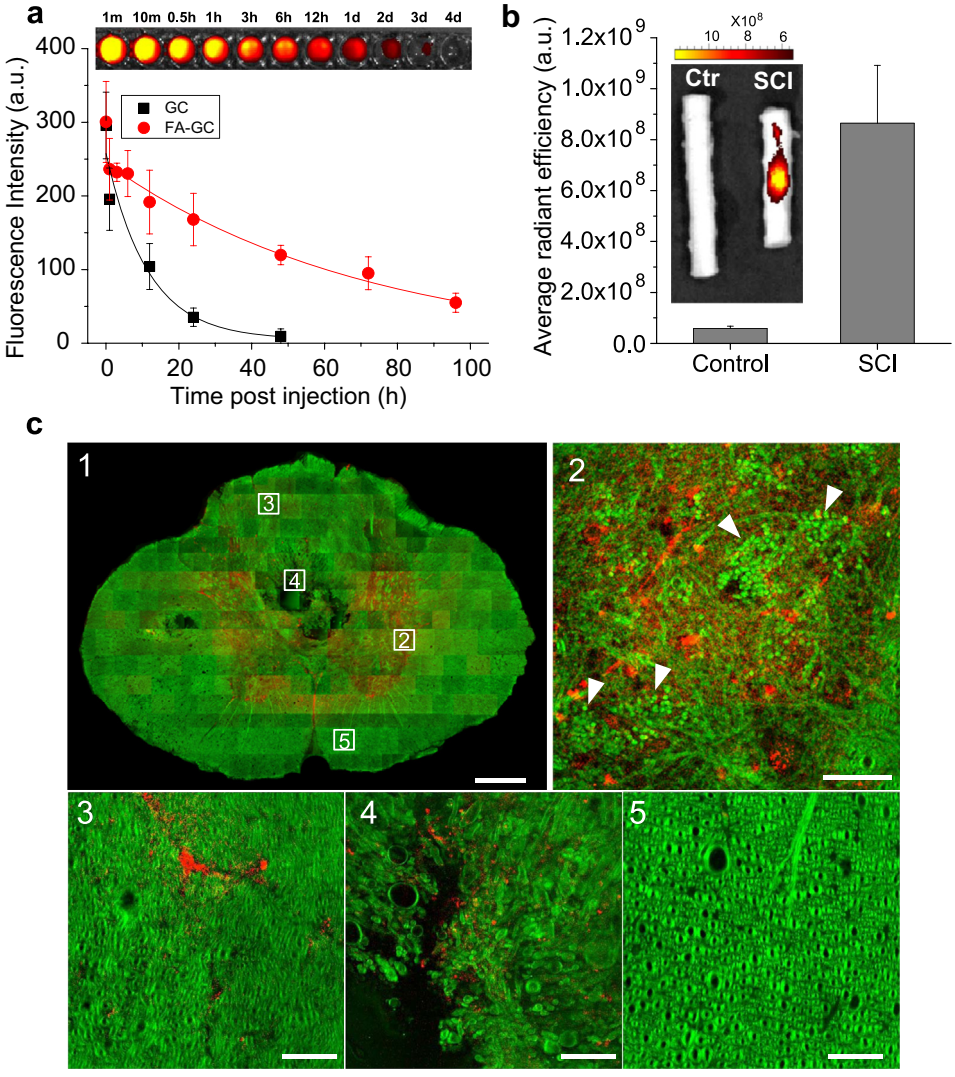

Fig. 3. FA–GC nanoparticles exhibited long blood retention time and targeted delivery to injured spinal cord. (a) Blood retention kinetics of FA–GC(-Cy5.5) and GC(-Cy5.5) in SCI rats. FA–GC(-Cy5.5) and GC(-Cy5.5) (both at 16 mg/kg, 1 ml in saline) were intravenously injected at 2 h post SCI. The data were fitted with a one-compartment model ($y = Ae^{(-x/t)} + y_0$). The fluorescence of FA–GC(-Cy5.5) in blood samples, drawn at different time points, were visualized (top). (b) Fluorescence imaging and quantification of FA–GC(-Cy5.5) in normal and injured spinal cords. (c) Distribution of FA–GC(-Cy5.5) in injured spinal cord. FA–GC and cord were visualized using two-photon fluorescence for Cy5.5 (red) and stimulated Raman loss signal from C–H vibration (green), respectively. A cross section through the injury epicenter shows the distribution of FA–GC (c1). Dotted squares represent high magnified images of the distribution of FA–GC (red) in the gray matter (c2), the dorsal funicular white matter (c3), the ventral portion of the dorsal funiculus (c4), and the ventral funiculus (c5). White arrows in c2 indicate packed red blood cells (Scale bar: 100 μm for C1 and 5 μm for c2-5). (For interpretation of the references to colour in this figure legend, the reader is referred to the web version of this article.)

Treatments were administrated at 2 h post injury by intravenous jugular vein injection. Bladder expression was manually carried out 3 times daily until reflex bladder emptying was established. The locomotor recovery was assessed using the Basso Beattie Bresnahan (BBB) locomotor rating score [38]. Two lab members conducted the test independently and agreement on the score was reached before the scores were finalized. The scores were recorded at day 1, 7, 14, 21, and 28. The locomotor behaviors were recorded via a video camera.

2.9. Immunofluorescence analysis of spinal cord tissue

At 28 days after the injury, the rats were anesthetized and transcardially exsanguinated with 150 ml physiological saline followed by fixation with 300 ml of ice-cold 4% paraformaldehyde in PBS (PH 7.4). A 1.5 cm thoracic spinal cord segment at the lesion center was dissected and then fixed 4 h by 4% paraformaldehyde in PBS (pH 7.4), and transferred to 30% sucrose in PBS (pH 7.4). The cord segments were embedded in tissue-embedding medium, and 30 μm sagittal sections were cut on a cryotome and mounted onto glass slides.

For immunofluorescence staining, the sections were permeabilized and blocked with 0.3% Triton X-100/10% normal goat serum (NGS) in PBS (pH 7.4) for 30 min. Primary antibodies were then applied to the sections overnight at 4 °C. Glia fibrillary acidic protein (GFAP, diluted 1:220, Abcam, Cambridge, MA, USA), ED-1 (diluted 1:50; Millipore, St. Charles, MO, USA) and SMI31 (diluted 1:500, Abcam, Cambridge, MA, USA) were used as the primary antibody to identify astrocyte and macrophage/activated microglia and axons, respectively. The sections were incubated the following day for 2 h at room temperature with secondary antibodies (Alexa Fluor 488, Invitrogen; Cy3, Invitrogen), washed, mounted, and then examined using an Olympus IX70 confocal microscope equipped with a FluoView program. The cavity volume measurement and 3D construction were conducted by a Neurolucida program, $GFAP^+$ and $ED\text{-}1^+$ fluorescence intensity were measured by Image J. The $SMI31^+$ axon number was counted manually by image J.

Luxol fast blue (LFB) staining was used to observe the spared myelin, the protocols have been described before [42]. The slides were dehydrated with 70% and 95% alcohol for 2 min each, and then they were immersed with 0.1% LFB solution at 37 °C for 4h. After cooling at 4 °C for 20 min, the slides were dipped in 95% alcohol 5 times and ddH_2O for 1 min, then they were cleared and sealed. To calculate the percentage of spared myelin, we firstly transferred the image to black, then we selected all the LFB stained area and measured it. After measuring the whole spinal cord area, we calculate the ratio of selected black area to the whole section area, which represent the percentage of spared myelin.

To define the cavity area, we performed hematoxylin and eosin (H&E) staining. Briefly, after drying the section, we stained the tissue in 50 ml conical tube filling with 0.1% hematoxylin, then the section was rinsed in cool running ddH_2O for 5 min. After dipping the section in 0.5% Eosin, we put the section in distilled H_2O, 50% alcohol, 70% alcohol, 95% alcohol, and 100% alcohol, then we dip the section in xylene several times, clean the slide, and seals it.

For assessment of axons, microphages, astrocyte, and myelin, four sections from FA–GC treated tissue and 3 sections from saline treated control group at epicenter were selected. For each section, three perilesion areas were chosen randomly to do the statistical analysis. Fluorescence intensity was used to represent the astrocyte, macrophages reaction, the axon number was counted to measure the spared axon, and the percentage of myelin stained area indicate the spared myelin. For the measurement of cavity volume percentage, 1 cm segment of thoracic spinal cord ($n = 3$ for each group) including the lesion epicenter was dissected and sectioned by transversely at 20 μm thickness by cryotome and mounted to glasses. 60 sections per each 1 cm length spinal cord were used to calculate the cavity volume, the whole spinal cord volume, and 3-dimensional reconstruction by Neurolucida software (MicroBrightfield, Inc.). The percentage of cavity volume to spinal cord volume was use to assess the neuroprotective effect of FA–GC nanoparticles.

2.10. In vivo toxicity analysis

Long-Evans adult male rats were randomized into the GC-FA nanoparticle-treated group ($n = 3$) or the saline-treated group ($n = 3$). Each rat (~300 g by weight) received 1 ml FA–GC nanoparticles (16 mg/kg in saline) or 1 ml saline solution through jugular vein injection. Blood samples (1 ml) were drawn through the jugular vein at day 1 and day 28 post treatment. Hematology and serum analysis were performed by Antech Diagnostics, Inc. in a blinded manner. The rats were then sacrificed and tissues including liver, lung, spleen, and kidneys were fixed in 10% neutral buffered formalin for at least 48 h, embedded into paraffin. Sections of 5 μm thickness were stained with hematoxylin and eosin in Purdue University Histopathology Lab. The slides were then examined on a Nikon microscope equipped with a charge-coupled device camera.

2.11. Statistical analysis

Values are expressed as mean ± SEM, and statistical comparisons between groups were made using the Student's *t*-test and a *P* value of <0.05 was considered significant.

3. Results

3.1. Physicochemical characteristics of FA–GC nanoparticles

Different amounts of FA (feed molar ratio of 45–180 mol FA to 1.0 mol GC) were conjugated to GC ($M_w = 250$ KDa) (Fig. 1a). With three different feed ratios of FA, FA–GC polymers with different degree of substitutions of FA were obtained, as listed in Table S1. The presence of FA in FA–GC polymer was confirmed by characteristic peaks at 6–8 ppm in ^1H NMR spectra (data not shown), and the amide linkage between GC and FA was confirmed by an increase in the amide peak at 1656 cm^{-1} in FT-IR spectra (Fig. 1b). Self-assembled FA–GC nanoparticles were generated by sonication in aqueous conditions. The zeta-potentials and average diameters of FA–GC nanoparticles were measured using a zeta-potential dynamic light scattering analyzer, respectively (Table S1). FA–GC nanoparticles showed similar positive zeta-potentials, implying the GC shell composes the nanoparticle surface. On the other hand, FA–GC nanoparticles with a degree of substitution of 12.8 had smaller diameter (236 nm) compared to other nanoparticles, and their spherical morphology was confirmed by transmission electron microscopy (Fig. 1c). Since smaller FA–GC nanoparticle size may allow more nanoparticles to accumulate at the injured spinal cord tissue, it was decided to use FA–GC nanoparticles with a degree of substitution of 12.8 in the following studies unless otherwise noted.

3.2. Neuroprotective effect of FA–GC nanoparticles against glutamate-induced excitotoxicity

Since glutamate level increase is the most significant pathological feature of SCI, we first confirmed the neuroprotective effect of FA–GC nanoparticles on primary spinal cord neuronal culture

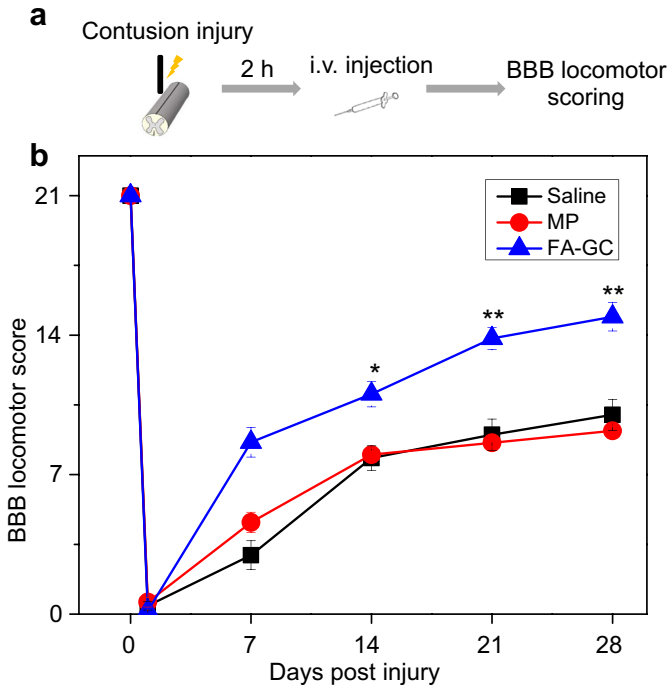

Fig. 4. FA–GC treatment promoted locomotor recovery after SCI. (a) Schematic diagram of experimental design. (b) BBB locomotor rating scale performed in rats that received saline ($n = 9$), methylprednisolone (MP, $n = 5$), and FA–GC ($n = 10$) at 2 h post SCI. Scores were recorded at day 1, 7, 14, and 28 post injury in a blinded manner. $^*P < 0.05$, $^{**}P < 0.01$.

using a glutamate-induced excitotoxicity model. In the control group, spinal cord neurons showed clear neuronal cell bodies and extended neurites (Fig. 2a, control, yellow arrow). After exposure to glutamate (Glu) for 24 h, neuronal loss and breakdown of neurites were clearly seen (Fig. 2a, Glu, red arrow). Pre-treatment by GC partially reduced neuronal loss and suppressed neurite degeneration (Fig. 2a, Glu + GC, yellow arrow). Pre-treatment by FA–GC nanoparticles showed greater effect on prevention of neuronal loss and neurite disintegration as compared to the use of GC alone (Fig. 2a, Glu + FA–GC, yellow arrow). Neuron viability percentage (%) was quantified using Hoechst/propidium iodide (PI) staining (Fig. 2a, right column). Administration of glutamate for 24 h led to massive neuronal loss and only 48% survived the glutamate insult. Pre-treatments by GC polymer or FA–GC nanoparticles significantly increased neuronal survival by 81% and 98%, respectively (Fig. 2b). These results demonstrate the neuroprotective effect of both GC and FA–GC nanoparticles. The better survival of neurons after FA–GC nanoparticle treatment than with the GC polymer treatment alone indicated the added neuroprotective effect of FA conjugation.

3.3. Pharmacokinetics and bioavailability of FA–GC nanoparticles in SCI animals

Next, we characterized the blood retention time and bioavailability of FA–GC nanoparticles for SCI using fluorescence labeling. As shown in Fig. 3a, FA–GC nanoparticles exhibited a long retention time in blood with a half-life of 20 h determined by a one-compartment model. In comparison, the non-modified GC polymer showed a half-life of 6 h. We also examined the bioavailability of FA–GC nanoparticles in injured and uninjured rat spinal cords at 1 day post injection. The fluorescence of Cy5.5 conjugated FA–GC nanoparticles was detected only at the lesion site of the injured spinal cord (Fig. 3b, insert). The non-injured spinal cord showed a background autofluorescence that was 15 times weaker compared to the FA–GC fluorescence in the injured cord.

To investigate cellular level localization of FA–GC nanoparticles in the injured spinal cord, we used two-photon excitation fluorescence and stimulated Raman loss microscopic imaging technology (Fig. 3c). FA–GC nanoparticles were highly accumulated in

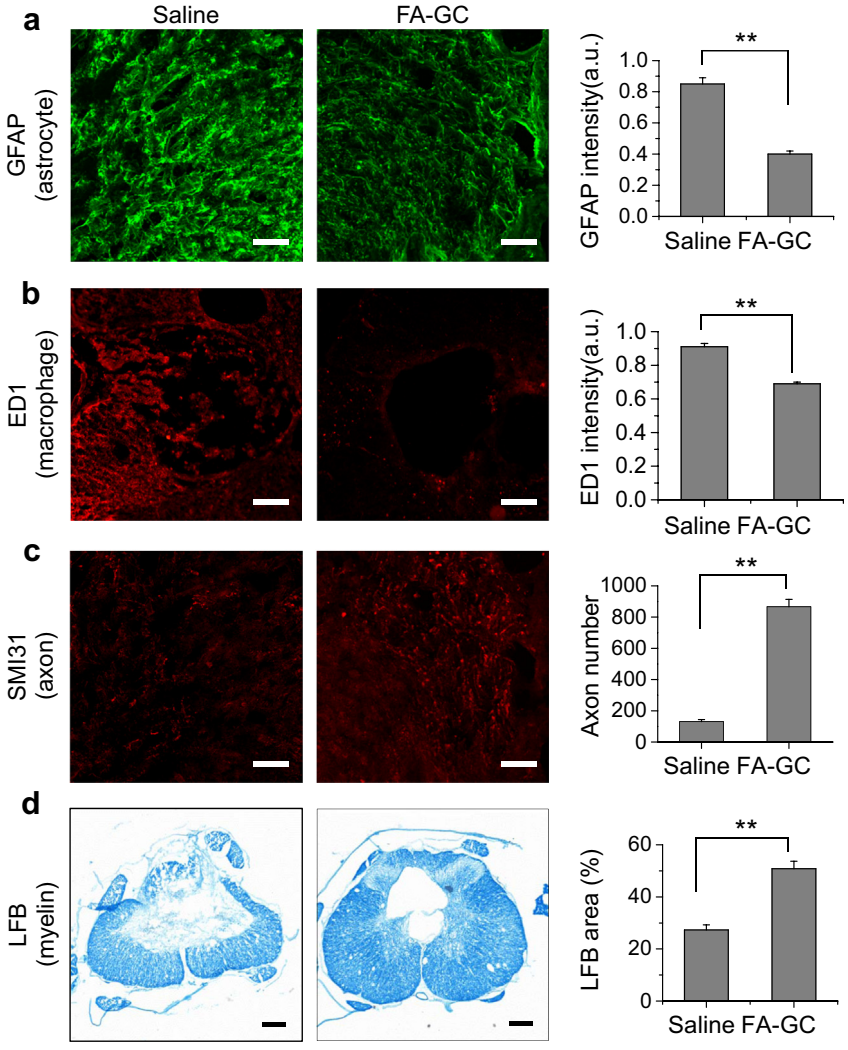

Fig. 5. FA–GC treatment improved histological outcomes. (a–b) Florescence images of GFAP+ and ED1+ cells in injured spinal cord at 28 day after saline and FA–GC treatments. The graphs right beside the image are the quantitative analysis of fluorescence intensity, showing FA–GC is capable of reduce the astrocyte and macrophage/microglia reaction. (c) Comparison of spared axons between two groups indicated by SMI31 stained axons, and the graph right beside the images is the quantitative number counting results, indicating an increased number of spared axons. (d) Luxol fast blue (LFB) staining of injured spinal cord for saline and FA–GC treated groups. The graph beside the images is the percentage of LFB staining area in the whole spinal cord. $^{**}P < 0.001$; $n = 3–4$ (scale bar: 100 μm). (For interpretation of the references to colour in this figure legend, the reader is referred to the web version of this article.)

the gray matter compared to the white matter at 1 d post injury (Fig. 3c–1). In the gray matter, aggregation of red blood cells and blood clots was observed, indicating blood vessel damages induced by contusive impact (Fig. 3c–2). FA–GC was present in the ventral portion of the dorsal funiculus, close to the central canal (Fig. 3c–4). The white matter was not seriously damaged as compare to gray matter (Fig. 3c–5). In fact, the ventral white matter remained morphologically intact with the absence of fluorescence of Cy5.5 conjugated FA–GC nanoparticles (Fig. 3c–5). Together, these results demonstrated selective accumulation of FA–GC nanoparticles at the lesion site.

3.4. Functional restoration of FA–GC nanoparticles in contusive SCI rats

To determine the effectiveness of FA–GC in functional recovery, we employed the Basso Beattie Bresnahan (BBB) locomotor rating scale to assess locomotor recovery in rats received intravenous injection of FA–GC nanoparticles. The control rats received either saline or MP injection. All injections were carried out at 2 h after contusive SCI, as shown schematically in Fig. 4a. The BBB scores were recorded at days 1, 7, 14, 21, and 28 after SCI in a blinded manner for all three groups (Fig. 4b). On day 28, an increase of 4.9 points in the BBB scale was seen in the FA–GC treated group compared to the saline treated group, and an increase of 5.7 points in the FA–GC treated group compared to the MP treated group (FA–GC: 14.9 ± 0.7, saline: 10.0 ± 0.7; MP: 9.2 ± 0.2). The score of 14.9 in the FA–GC treated group indicates consistent weight-supported plantar steps and frequent forelimb-hindlimb coordination, whereas the BBB scores of 9–10 in the MP and saline groups mean that the rats were only able to achieve weight support in stance and there was no coordination between fore- and hindlimbs (Videos S1, S2).

Supplementary video related to this article can be found at http://dx.doi.org/10.1016/j.biomaterials.2013.11.074.

3.5. Histological improvement of injured spinal cord by FA–GC treatment

To determine the anatomical basis of observed functional recovery, we examined several key parameters that were associated with tissue damage and repair. These parameters included densities of axons, astrocytes, macrophages, myelin, and volumes of cavity at day 28 post injury. Astrocytes, which play a major role in the formation of gliosis after SCI [43], were visualized using glial fibrillary acidic protein (GFAP) antibodies. The immunoreactivity of GFAP in the FA–GC group was 50% of that in the saline group (Fig. 5a), indicating that FA–GC treatment reduced astrogliosis at the lesion site. The macrophages play a major role in inflammatory responses including modulating axon degeneration and myelin clearance after SCI [44]. Measured by ED1 immunofluorescence, FA–GC treatment decreased the density of macrophages by 24% compared to the saline treated group (Fig. 5b). To determine whether the reduced immunoreactivity of astrocytes and macrophages benefit the survival of axons and myelin, we quantified their densities using SMI31 immunofluorescence and luxol fast blue

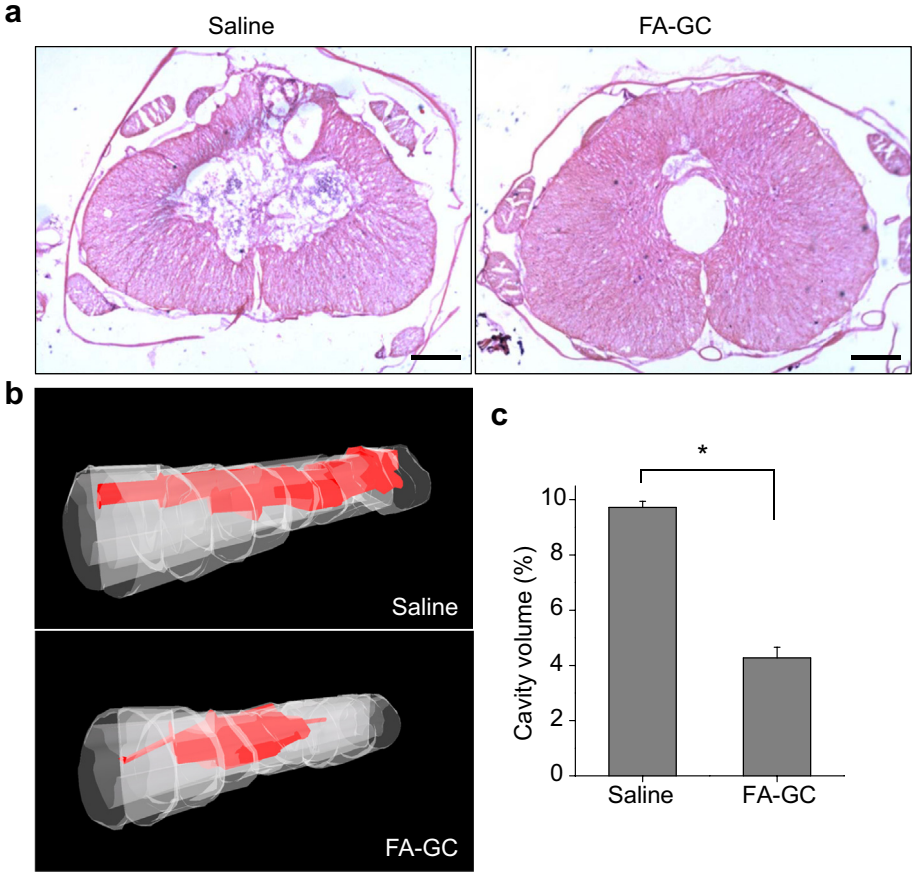

Fig. 6. FA–GC nanoparticles reduces cavitation following T10 contusion SCI. (a) Spinal cord harvest 4 weeks post-SCI showed reduced cavitation through hematoxylin and eosin (H&E) staining with FA–GC treatment compare to saline treated animals. (b) 3D reconstruction of cavity volume from representative cases indicating the neuroprotective effects of FA–GC nanoparticles. (c) Quantification of cavity volume, illustrating the significantly decreased cavity volume in FA-GC treated animals compare to saline control. $^{*}P < 0.05$; $n = 3$ (scale bar: 100 μm).

staining, respectively. Compared to the saline treated group, FA–GC treatment increased the number of spared axons in the epicenter of the spinal cord by 6.6 times (Fig. 5c) and enlarged the luxol fast blue stained area by 2 times (Fig. 5d). These results collectively show that FA–GC treatment not only suppressed astrogliosis and inflammation, but also protected axons and myelin.

In accordance with the cellular responses described above, administration of FA–GC nanoparticles reduced the volume of the lesion cavity (Fig. 6a) as compared to the saline treated group. By hematoxylin and eosin (H&E) staining and employing the Neurolucida system, we reconstructed the spinal cord sections into 3D images and determined the cavity volume (Fig. 6b). The cavity volume of the FA–GC treated group was 2.3 times smaller than that of the saline treated group (Fig. 6c). The reduced cavitation further supports the neuroprotective effect of FA–GC nanoparticles.

3.6. *In vivo* toxicity analysis

We have evaluated both acute and chronic toxicity of FA–GC nanoparticle administration to Long-Evans rats through blood and histological analyses. After saline and FA–GC administrations to rats, blood samples were collected at day 1 and day 28 for acute and chronic toxicity evaluation, respectively. The results of hematology and serum analyses between the FA–GC group and saline treated group were not significantly different (Fig. 7a). The levels of creatinine and alanine transaminase for the FA–GC group were the

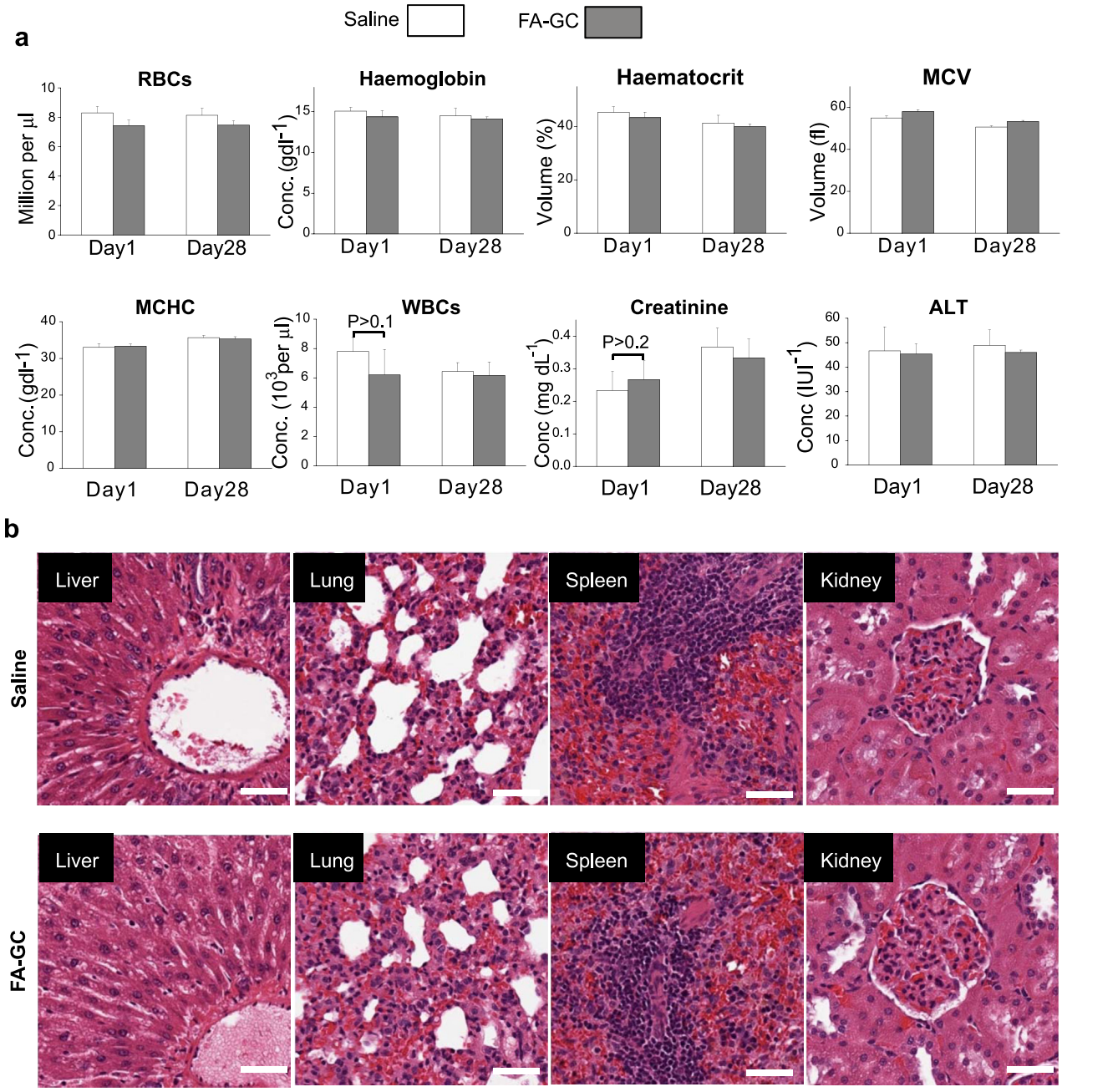

Fig. 7. *In vivo* toxicity analysis. (a) Complete blood count and serum analysis of Long-Evans rats at day 1 and day 28 following injection of saline solution (1 ml) or d FA–GC nanoparticles (16 mg/kg, 1 ml in saline). White column: saline. Gray column: FA–GC nanoparticles. (b) Histological analysis of explanted liver, lung, spleen, and kidney stained with hematoxylin and eosin (scale bar: 50 µm).

same as that of the saline group, indicating no damage to the kidney and the liver. The morphology of vital organs was also assessed using H&E staining. No morphological difference was observed between the groups treated with saline and FA–GC at day 28 post treatment (Fig. 7b). Together, these results revealed no adverse effects of FA–GC nanoparticles in the rat model.

4. Discussion

After primary SCI, protection of neurons and glial cells from secondary degeneration is crucial for functional recovery. Currently, methylprednisolone (MP), a steroid drug, is the only option for early pharmacological treatment of SCI, although its therapeutic effect is controversial. Using non-cytotoxic and neuroprotective nanoparticles reported here opens a new opportunity for effective treatment of SCI. Systemic administration of the FA–GC nanoparticles at 2 h-post SCI significantly restored locomotor function compared to MP administration. Theses outcomes demonstrated superior therapeutic effects and increased time window of FA–GC nanoparticles for SCI treatment as compared to other nanomaterials using non-functional and synthetic polymers such as PEG and Poloxamer [19,45].

FA conjugation to GC polymer enhanced not only the neuroprotective effect, but also modified the pharmacological properties. The FA–GC polymer formed self-assembled nanoparticles, and the nanoparticles demonstrated a long retention time in the blood stream by intravenously administration, compared to GC polymer alone. Moreover, the FA–GC nanoparticles efficiently accumulated to the injury site particularly in the gray matter region which is highly vulnerable to an injury insult. The FA–GC nanoparticles reached the lesion site likely through the ruptured blood capillaries and interrupted brain-spinal cord-barriers. Gray matter in the spinal cord, consisting of neuronal cell bodies, glial cells, and capillaries, routes sensory or motor stimulus to interneurons of the central nervous system [46]. Strong-impact force to the spinal cord can easily break small blood vessels and damage the blood–spinal cord barrier in the gray matter that may cause ischemia and neuronal cell apoptosis [47]. Consequently, secondary degeneration spreads from the gray matter to the white matter [48,49]. This pathological progression damages not only neurons and glial cells in the gray matter, but also axons and myelin in the white matter. Targeted delivery of FA–GC nanoparticles into injured gray matter prevented such progression at an early stage, thereby protecting axons and myelin in the white matter that transmit locomotor signaling. This mechanism could account for the significant locomotor functional recovery enabled by FA–GC treatment.

Although various polymers or nanomaterials have been used for early SCI treatment, they had to be administrated within a short period (less than 15 min) after SCI or even before SCI to achieve distinct therapeutic effect [23,50–52]. Such time windows are not clinically relevant for clinical SCI treatment because it generally requires at least 1 or 2 h for patient transfer to an emergency department and diagnostic assessment before initial treatment. In this study, we demonstrated a marked therapeutic effect of FA–GC nanoparticles, both histologically and behaviorally, by systemic administration of FA–GC nanoparticle at 2 h post injury. Our results indicate the promising potential of FA–GC nanoparticles for treating SCI in clinical settings. Moreover, because intravenous administration is simple to implement, our approach is applicable to treat SCI in the field. Notably, we only treated SCI rats at fixed dose of FA–GC nanoparticles at 2 h post the injury in this pilot study. Further work is needed to validate the effectiveness by assessing preclinical outcomes in terms of animal species, dosage, therapeutic time window, and severity of injuries.

5. Conclusions

We have shown high neuroprotective effects of ferulic acid (FA)–glycol chitosan (GC) nanoparticles against spinal cord injury (SCI) with a clinically relevant therapeutic time window. The systemic administration of FA–GC nanoparticles significantly rescued axons and neuron cells at the lesion site, while the number of activated astrocytes and macrophages decreased. These neuroprotective effects consequently led functional recovery following SCI.

Acknowledgments

This work was supported by a translational research grant from the Wallace H. Coulter Foundation, NIH R01 CA129287 to KP and JXC, NS059622 and NS050243 to XMX, CDMRP W81XWH-12-1-0562 to XMX and JXC, NSF CHE 0847205 and NIH 8R21GM103454 to ZO. The authors thank Dr. Xiaofei Wang for kind help in surgery, Dr. Kwangmeyung Kim for providing the Cy5.5 dyes, and Dr. Mark Cisneros for critical reading of the manuscript.

Appendix A. Supplementary data

Supplementary data related to this article can be found at http://dx.doi.org/10.1016/j.biomaterials.2013.11.074.

References

[1] Thuret S, Moon LDF, Gage FH. Therapeutic interventions after spinal cord injury. Nat Rev Neurosci 2006;7:628–43.
[2] Bradbury EJ, McMahon SB. Spinal cord repair strategies: why do they work? Nat Rev Neurosci 2006;7:644–53.
[3] Liu NK, Xu XM. Phospholipase A2 and its molecular mechanism after spinal cord injury. Mol Neurobiol 2010;41:197–205.
[4] Simon CM, Sharif S, Tan RP, LaPlaca MC. Spinal cord contusion causes acute plasma membrane damage. J Neurotrauma 2009;26:563–74.
[5] Klussmann S, Martin-Villalba A. Molecular targets in spinal cord injury. J Mol Med 2005;83:657–71.
[6] Ducker TB, Kindt GW, Kempe LG. Pathological findings in acute experimental spinal cord trauma. J Neursurg 1971;35:700–8.
[7] Bracken MB, Shepard MJ, Collins WF, Holford TR, Young W, Baskin DS, et al. A randomized, controlled trial of methylprednisolone or naloxone in the treatment of acute spinal-cord injury. N Engl J Med 1990;322:1405–11.
[8] Yan P, Xu J, Li Q, Chen S, Kim G-M, Hsu CY, et al. Glucocorticoid receptor expression in the spinal cord after traumatic injury in adult rats. J Neurosci 1999;19:9355–63.
[9] Ito Y, Sugimoto Y, Tomioka M, Kai N, Tanaka M. Does high dose methylprednisolone sodium succinate really improve neurological status in patient with acute cervical cord injury?: a prospective study about neurological recovery and early complications. Spine 2009;34:2121–4.
[10] Tsutsumi S, Ueta T, Shiba K, Yamamoto S, Takagishi K. Effects of the second national acute spinal cord injury study of high-dose methylprednisolone therapy on acute cervical spinal cord injury–results in spinal injuries center. Spine 2006;31:2992–6.
[11] Saracino GAA, Cigognini D, Silva D, Caprini A, Gelain F. Nanomaterials design and tests for neural tissue engineering. Chem Soc Rev 2013;42:225–62.
[12] Kubinová Š, Syková E. Nanotechnology for treatment of stroke and spinal cord injury. Nanomedicine 2009;5:99–108.
[13] Cho Y, Shi R, Borgens R, Ivanisevic A. Repairing the damaged spinal cord and brain with nanomedicine. Small 2008;4:1676–81.
[14] Chvatal SA, Kim Y-T, Bratt-Leal AM, Lee H, Bellamkonda RV. Spatial distribution and acute anti-inflammatory effects of methylprednisolone after sustained local delivery to the contused spinal cord. Biomaterials 2008;29:1967–75.
[15] Tysseling-Mattiace VM, Sahni V, Niece KL, Birch D, Czeisler C, Fehlings MG, et al. Self-assembling nanofibers inhibit glial scar formation and promote axon elongation after spinal cord injury. J Neurosci 2008;28:3814–23.
[16] Wang YC, Wu YT, Huang HY, Lin HI, Lo LW, Tzeng SF, et al. Sustained intraspinal delivery of neurotropic factor encapsulated in biodegradable nanoparticles following contusive spinal cord injury. Biomaterials 2008;29:4546–53.
[17] Cho Y, Borgens RB. Polymer and nano-technology applications for repair and reconstruction of the central nervous system. Exp Neurol 2012;233:126–44.
[18] Friedman JA, Windebank AJ, Moore MJ, Spinner RJ, Currier BL, Yaszemski MJ. Biodegradable polymer grafts for surgical repair of the injured spinal cord. Neurosurgery 2002;51:742–52.

[19] Borgens RB, Shi R, Bohnert D. Behavioral recovery from spinal cord injury following delayed application of polyethylene glycol. J Exp Biol 2002;205:1–12.
[20] Shi R, Borgens RB. Acute repair of crushed guinea pig spinal cord by polyethylene glycol. J Neurophysiol 1999;81:2406–14.
[21] Marks JD, Pan CY, Bushell T, Cromie W, Lee RC. Amphiphilic, tri-block copolymers provide potent, membrane-targeted neuroprotection. FASEB J 2001;15:1107–9.
[22] Follis F, Jenson B, Blisard K, Hall E, Wong R, Kessler R, et al. Role of poloxamer 188 during recovery from ischemic spinal cord injury: a preliminary study. J Invest Surg 1996;9:149–56.
[23] Shi Y, Kim S, Huff TB, Borgens RB, Park K, Shi R, et al. Effective repair of traumatically injured spinal cord by nanoscale block copolymer micelles. Nat Nano 2010;5:80–7.
[24] Cheng CY, Su SY, Tang NY, Ho TY, Lo WY, Hsieh CL. Ferulic acid inhibits nitric oxide-induced apoptosis by enhancing GABAB1 receptor expression in transient focal cerebral ischemia in rats. Acta Pharmacol Sin 2010;31:889–99.
[25] Ratih P, Kim S-K. Neuroprotective properties of chitosan and its derivatives. Marine Drugs 2010;8:2117–28.
[26] Koh P-O. Ferulic acid attenuates the injury-induced decrease of protein phosphatase 2A subunit B in ischemic brain injury. PLoS ONE 2013;8:e54217.
[27] Cheng CY, Su SY, Tang NY, Ho TY, Chiang SY, Hsieh CL. Ferulic acid provides neuroprotection against oxidative stress-related apoptosis after cerebral ischemia/reperfusion injury by inhibiting ICAM-1 mRNA expression in rats. Brain Res 2008;1209:136–50.
[28] Lin TY, Lu CW, Huang S-K, Wang S-J. Ferulic acid suppresses glutamate release through inhibition of voltage-dependent calcium entry in rat cerebrocortical nerve terminals. J Med Food 2013;16:112–9.
[29] Srinivasan M, Sudheer AR, Menon VP. Ferulic acid: therapeutic potential through its antioxidant property. J Clin Biochem Nutr 2007;40:92–100.
[30] Graf E. Antioxidant potential of ferulic acid. Free Radic Biol Med 1992;13:435–48.
[31] Cho Y, Shi RY, Borgens RB. Chitosan produces potent neuroprotection and physiological recovery following traumatic spinal cord injury. J Exp Biol 2010;213:1513–20.
[32] Liu HT, Li WM, Xu G, Li XY, Bai XF, Wei P, et al. Chitosan oligosaccharides attenuate hydrogen peroxide-induced stress injury in human umbilical vein endothelial cells. Pharmacol Res 2009;59:167–75.
[33] Li J, He J, Yu C. Chitosan oligosaccharide inhibits LPS-induced apoptosis of vascular endothelial cells through the BKCa channel and the p38 signaling pathway. Int J Mol Med 2012;30:157–64.
[34] Zhou SL, Yang YM, Gu XS, Ding F. Chitooligosaccharides protect cultured hippocampal neurons against glutamate-induced neurotoxicity. Neurosci Lett 2008;444:270–4.
[35] Je JY, Kim SK. Reactive oxygen species scavenging activity of aminoderivatized chitosan with different degree of deacetylation. Bioorg Med Chem 2006;14:5989–94.
[36] Lee HJ, Park J, Yoon OJ, Kim HW, Lee DY, Kim DH, et al. Amine-modified single-walled carbon nanotubes protect neurons from injury in a rat stroke model. Nat Nano 2011;6:121–5.
[37] Na JH, Lee S-Y, Lee S, Koo H, Min KH, Jeong SY, et al. Effect of the stability and deformability of self-assembled glycol chitosan nanoparticles on tumor-targeting efficiency. J Control Release 2012;163:2–9.
[38] Basso DM, Beattie MS, Bresnahan JC. A sensitive and reliable locomotor rating scale for open field testing in rats. J Neurotrauma 1995;12:1–21.
[39] Jiang XY, Fu SL, Nie BM, Li Y, Lin L, Yin L, et al. Methods for isolating highly-enriched embryonic spinal cord neurons: a comparison between enzymatic and mechanical dissociations. J Neurosci Methods 2006;158:13–8.
[40] Basso DM, Beattie MS, Bresnahan JC. Graded histological and locomotor outcomes after spinal cord contusion using the NYU weight-drop device versus transection. Exp Neurol 1996;139:244–56.
[41] Zhang D, Slipchenko MN, Cheng J-X. Highly sensitive vibrational imaging by femtosecond pulse stimulated Raman loss. J Phys Chem Lett 2011;2:1248–53.
[42] Iannotti C, Ping Zhang Y, Shields CB, Han Y, Burke DA, Xu XM. A neuroprotective role of glial cell line-derived neurotrophic factor following moderate spinal cord contusion injury. Exp Neurol 2004;189:317–32.
[43] Fitch MT, Silver J. CNS injury, glial scars, and inflammation: inhibitory extracellular matrices and regeneration failure. Exp Neurol 2008;209:294–301.
[44] Popovich P, McTigue D. Damage control in the nervous system: beware the immune system in spinal cord injury. Nat Med 2009;15:736–7.
[45] Borgens RB, Bohnert D, Duerstock B, Spomar D, Lee RC. Subcutaneous tri-block copolymer produces recovery from spinal cord injury. J Neurosci Res 2004;76:141–54.
[46] Nahin RL, Madsen AM, Giesler GJ. Anatomical and physiological studies of the gray matter surrounding the spinal cord central canal. J Comp Neurol 1983;220:321–35.
[47] Dumont RJ, Okonkwo DO, Verma S, Hurlbert RJ, Boulos PT, Ellegala DB, et al. Acute spinal cord injury, part I: pathophysiologic mechanisms. Clin Neuropharmacol 2001;24:254–64.
[48] David S, Kroner A. Repertoire of microglial and macrophage responses after spinal cord injury. Nat Rev Neurosci 2011;12:388–99.
[49] Hagg T, Oudeag M. Degenerative and spontaneous regenerative processes after spinal cord injury. J Neurotrauma 2006;23:263–80.
[50] Dugan LL, Turetsky DM, Du C, Lobner D, Wheeler M, Almli CR, et al. Carboxyfullerenes as neuroprotective agents. Proc Natl Acad Sci U S A 1997;94:9434–9.
[51] Kim YT, Caldwell J-M, Bellamkonda RV. Nanoparticle-mediated local delivery of methylprednisolone after spinal cord injury. Biomaterials 2009;30:2582–90.
[52] Chen CL, Chang SF, Lee D, Yang LY, Lee YH, Hsu C, et al. Bioavailability effect of methylprednisolone by polymeric micelles. Pharm Res 2008;25:39–47.